

Aberystwyth University

Glacitectonic deformation in the Chuos Formation of northern Namibia

Busfield, Marie E.; Le Heron, Daniel P.

Published in:

Proceedings of the Geologists' Association

DOI:

[10.1016/j.pgeola.2012.10.005](https://doi.org/10.1016/j.pgeola.2012.10.005)

Publication date:

2013

Citation for published version (APA):

Busfield, M. E., & Le Heron, D. P. (2013). Glacitectonic deformation in the Chuos Formation of northern Namibia: Implications for neoproterozoic ice dynamics. *Proceedings of the Geologists' Association*, 124(5), 778-789. <https://doi.org/10.1016/j.pgeola.2012.10.005>

General rights

Copyright and moral rights for the publications made accessible in the Aberystwyth Research Portal (the Institutional Repository) are retained by the authors and/or other copyright owners and it is a condition of accessing publications that users recognise and abide by the legal requirements associated with these rights.

- Users may download and print one copy of any publication from the Aberystwyth Research Portal for the purpose of private study or research.
- You may not further distribute the material or use it for any profit-making activity or commercial gain
- You may freely distribute the URL identifying the publication in the Aberystwyth Research Portal

Take down policy

If you believe that this document breaches copyright please contact us providing details, and we will remove access to the work immediately and investigate your claim.

tel: +44 1970 62 2400
email: is@aber.ac.uk

Manuscript Number: PGEOLA-D-12-00028R1

Title: Glacitectonic deformation in the Chuos Formation of northern
Namibia: implications for Neoproterozoic ice dynamics

Article Type: Special Issue: Glacitectonics

Keywords: Neoproterozoic; glacitectonism; ductile deformation; Snowball
Earth; Otavi Mountainland

Corresponding Author: Miss Marie Elen Busfield,

Corresponding Author's Institution: Royal Holloway

First Author: Marie Elen Busfield

Order of Authors: Marie Elen Busfield; Daniel P Le Heron

Abstract: The Chuos Formation is a diamictite-dominated succession of Cryogenian age, variously interpreted as the product of glaciomarine deposition, glacially-related mass movement, or rift-related sediment remobilisation in a non-glacial environment. These interpretations have wide ranging implications for the extent of ice cover during the supposedly pan-global Neoproterozoic icehouse. In the Otavi Mountainland, northern Namibia, detailed analysis of soft sediment deformation structures on the macro- and micro-scale support glacitectonic derivation in response to overriding ice from the south/south-east. Overall, the upward increase in strain intensity, predominance of ductile deformation features (e.g. asymmetric folds, rotational turbates and necking structures, clast boudinage, unistrial plasmic fabrics) and pervasive glacitectonic lamination support subglacial deformation under high and sustained porewater pressures. In contrast, soft sediment structures indicative of mass movements, including flow noses, tile structures, and basal shear zones, are not present. The close association of subglacial deformation, abundant ice-rafted debris and ice-contact fan deposits indicate subaqueous deposition in an ice-proximal setting, subject to secondary subglacial deformation during oscillation of the ice margin. These structures thus reveal evidence of dynamic grounded ice sheets in the Neoproterozoic, demonstrating their key palaeoclimatic significance within ancient sedimentary successions.

1 Glacitectonic deformation in the Chuos Formation of northern Namibia:
2 implications for Neoproterozoic ice dynamics

3
4
5
6
7
8
9
10 Marie E Busfield^{1*} & Daniel P Le Heron¹

11
12 ¹*Department of Earth Sciences, Royal Holloway, University of London, Egham, Surrey,*
13
14 *TW20 0EX*
15
16

17
18
19 *Corresponding author. E-mail: Marie.Busfield.2011@live.rhul.ac.uk
20
21

22 **Abstract**
23
24

25 The Chuos Formation is a diamictite-dominated succession of Cryogenian age, variously
26
27 interpreted as the product of glaciomarine deposition, glacially-related mass movement, or
28
29 rift-related sediment remobilisation in a non-glacial environment. These interpretations have
30
31 wide ranging implications for the extent of ice cover during the supposedly pan-global
32
33 Neoproterozoic icehouse. In the Otavi Mountainland, northern Namibia, detailed analysis of
34
35 soft sediment deformation structures on the macro- and micro-scale support glacitectonic
36
37 derivation in response to overriding ice from the south/south-east. Overall, the upward
38
39 increase in strain intensity, predominance of ductile deformation features (e.g. asymmetric
40
41 folds, rotational turbates and necking structures, clast boudinage, unistrial plasmic fabrics)
42
43 and pervasive glacitectonic lamination support subglacial deformation under high and
44
45 sustained porewater pressures. In contrast, soft sediment structures indicative of mass
46
47 movements, including flow noses, tile structures, and basal shear zones, are not present. The
48
49 close association of subglacial deformation, abundant ice-rafted debris and ice-contact fan
50
51 deposits indicate subaqueous deposition in an ice-proximal setting, subject to secondary
52
53 subglacial deformation during oscillation of the ice margin. These structures thus reveal
54
55 evidence of dynamic grounded ice sheets in the Neoproterozoic, demonstrating their key
56
57 palaeoclimatic significance within ancient sedimentary successions.
58
59
60
61
62
63
64
65

1. Introduction

The concept of a Neoproterozoic icehouse has remained contentious since its inception in the early 19th century (*‘die Eiszeit’* of Agassiz, 1837: cf. Allen and Etienne, 2008), with renewed deliberation in recent years following proposal of the ‘snowball Earth’ hypothesis (Kirschvink, 1992; Hoffman et al., 1998; Hoffman and Schrag, 2002). This hypothesis has centred on the recognition of broadly age-equivalent diamictite-dominated successions on each continent, which are argued to be glaciogenic in origin (Hoffman et al., 1998; Hoffman and Schrag, 2002). Many diamictites are sharply overlain by dolomitized carbonates, interpreted as the record of rapid post-glacial climatic recovery (Shields, 2005). Compared to younger icehouse intervals, diagnostic glacial indicators, including striated and faceted clasts, subglacially striated pavements and extrabasinal clast assemblages, are notably scarce in the Neoproterozoic (Etienne et al., 2007), and rarely occur together in any one glacial succession. Consequently, Neoproterozoic diamictites have been argued to represent non-glacial, syn-tectonic sediment gravity flows (e.g. Eyles and Januszcak, 2004, 2007), associated with widespread rift activity during break-up of the Rodinia supercontinent.

In Quaternary studies, detailed analysis of soft-sediment deformation structures has received significant credence in discriminating between glacial and non-glacial successions (e.g. Lachniet et al., 2001; Menzies and Zaniewski, 2003; van der Meer and Menzies, 2011). However, with a few notable exceptions (e.g. Benn and Prave, 2006; Arnaud, 2008, 2012), such analyses are scarcely applied to Neoproterozoic deposits. To redress this, we present a new macro- and micro-scale structural analysis of the Chuos Formation of Cryogenian age in the Otavi Mountainland, northern Namibia (Fig. 1). The study will utilise standard sedimentological and structural analysis of the diamictite succession in order to determine the

genetic origin of the Chuos Formation, and assess the significance of soft-sediment deformation structures as palaeoclimate proxies during Neoproterozoic glaciation.

1.1 Geological background

The Otavi Group is a carbonate-dominated succession of Neoproterozoic age housing two diamictite horizons, the older Chuos and younger Ghaub formations (Fig. 1), each sharply overlain by fine-grained carbonate deposits (Hoffmann & Prave, 1996; Hoffman & Halverson, 2008; Miller, 2008). These horizons have been dated in turn to $<746 \pm 2$ Ma (Hoffman et al., 1996) and 635.5 ± 1.2 Ma (Hoffmann et al., 2004), through U-Pb zircon ages of underlying and interbedded volcanic ash beds, leading to correlation with the purportedly global Sturtian and Marinoan glaciations, respectively (Kennedy et al., 1998). In light of the argued syn-rift derivation of the diamictite assemblages (e.g. Eyles & Januszczyk, 2004, 2007), proponents of the glacial hypothesis have focussed largely on the younger Ghaub Formation, considered to have accumulated during the ‘drift’ stage of post-rift subsidence (Hoffman & Halverson, 2008). The older Chuos Formation, by comparison, has received less attention.

The glacial origin of the Chuos Formation was first proposed by Gevers (1931) due to its lithological similarity to the Late Palaeozoic Dwyka Tillite (cf. Henry et al., 1986), and its abundance of faceted and extrabasinal clasts. The stratigraphic position of the Chuos between carbonate successions was used to support a glaciomarine origin (Martin 1965a, b; Hedberg 1979), in-keeping with the regional absence of subglacial striated pavements (Kroner & Rankama, 1973). Alternative studies conversely describe the textural immaturity of the diamictites, abundance of locally-derived erratic lithologies and their spatial and temporal association with faults as evidence of high energy, rift-related submarine gravity flow deposition (e.g. Hedberg, 1979; Miller 1983; Porada, 1983; Porada & Wittig 1983a, b; Martin

et al., 1985). Under this scenario, the abundant outsized clasts, frequently cited as evidence of ice-rafting (e.g. Hoffman et al., 1998), are interpreted as the product of local mass flow ‘rafting’, or gravitational settling from overlying diamictites (Martin et al., 1985; Eyles & Januszczak, 2007). Further models propose a compromise between these two hypotheses, wherein both glacial deposition and gravitationally driven mass flows interact within an ice marginal, glaciomarine environment (Hoffmann, 1983; Henry et al. 1986).

Three interpretations of the diamictites are thus possible: 1) those generated directly by glacial processes; 2) those of primary glacial origin but re-worked by gravitational mass transport; and, 3) those generated by mass flow or slope failure without glacial influence. Consequently, criteria to correctly distinguish these environments remain pivotal to the debate surrounding the origin of the Chuos Formation. These criteria, in turn, have wide implications for interpretations of Neoproterozoic diamictites from a global perspective.

1.2. Study area and stratigraphy

The Otavi Mountainland in northern Namibia exposes a thick succession of Neoproterozoic strata flanking the southern margin of the Owambo Basin (Fig. 1). The Chuos Formation exhibits considerable lateral thickness variations across the region, reaching up to 130 m in the central and western sectors, and pinching out towards the south-east (Hoffmann & Prave, 1996). In the study area, on Ghaub and Varianto farms (Fig. 2), it rests with angular unconformity on sandstones and conglomerates of the Nosib Group (here the Nabis Formation; Miller, 2008), and is sharply overlain by fine-grained carbonate mudstone of the Berg Aukas Formation. The study area is ideally situated in the least deformed northern margin of the Damara Orogenic Belt, characterised by a low shear, fold-thrust zone and sub-greenschist facies metamorphism (Gray et al., 2008; Miller, 2008). These characteristics

1 97 permit detailed sedimentological and structural analysis of the diamictite horizons as they
2 98 have suffered minimal tectonic and metamorphic overprint.
3
4

5 99 **2. Methodology**

6
7
8 100 Sedimentary logging of the Chuos Formation was undertaken at several exposures across the
9 101 Ghaub and Varianto Farms at a metre-scale resolution. This process determined upper and
10 102 lower boundary relationships, enabling thickness changes to be documented across the area,
11 103 and the internal architecture of the formation to be characterised in detail. Lithofacies were
12 104 described on the macro-scale, including clast fabrics, bedding relationships, and the presence
13 105 and orientation of deformation structures.
14
15

16 106 For the purpose of this study, micro-scale analysis is restricted to an exposure of highly
17 107 deformed diamictite, where vertical changes in deformation style could be documented in
18 108 detail. Oriented samples were collected at appropriate intervals for thin section analysis,
19 109 determined where macro-scale changes in sedimentary or structural features were apparent.
20 110 Thin section analysis was undertaken using a petrographic microscope at low magnification
21 111 (1x and 2x), under plane and cross-polarized light, as well as examining high resolution
22 112 photographs and digital scans. Micro-scale features were described using standard structural
23 113 terminology and micromorphological techniques (*sensu* van der Meer, 1987, 1993; Menzies,
24 114 2000; Carr, 2004).
25
26

27 115 **3. Sedimentology**

28 116 **3.1. Description**

29 117 Three principal facies can be recognized comprising: 1) stratified diamictite facies, 2) sheared
30 118 and laminated diamictite, and 3) massive diamictite facies. In the south-east of the study area
31 119 the latter facies dominates (Fig. 2), with intercalated and overlying units of stratified and
32
33
34
35
36
37
38
39
40
41
42
43
44
45
46
47
48
49
50
51
52
53
54
55
56
57
58
59
60
61
62
63
64
65

sheared diamictite becoming more abundant northwards. At outcrop scale, diamictite units typically coarsen upwards, although grading is rarely observed within individual beds. Clast lithologies consist predominantly of well rounded quartzite, with minor sub-angular to rounded mudstone, mica schist, granite gneiss and andesite. Striated and faceted clasts were not observed. Evidence of impact-related deformation beneath some of the larger outsized clasts is typically restricted to the stratified units, expressed through puncturing and downwarping of the underlying laminae (Fig. 3a). This facies also preserves large-scale (1-2 m) eastward-dipping foreset structures (Log 2; Fig. 2), overlain by a series of soft-sediment striated surfaces, comprising centimetre-scale linear grooves and ridges which trend approximately north-south along exposed bedding planes (Fig. 3c). Detailed description of deformation structures within the sheared and laminated facies will be discussed in section 4 below.

4. Deformation structures

A spectacularly well exposed vertical section of the Chuos Formation containing approximately 30 m of highly deformed and attenuated diamictite crops out on Varianto Farm (GR 19°24'415 S, 17°42'443 E; Fig. 2), in the central portion of the Otavi Mountainland. The sequence overlies coarse sandstone of the Nabis Formation. These deposits exhibit well developed convolute bedding and soft-sediment fold structures approximately 6 m below the boundary with the Chuos, passing upwards into undeformed, well bedded sandstone units (Log 3; Fig. 2). Likewise, finely laminated carbonate mudstone of the Berg Aukas Formation, sharply overlying the Chuos Formation, is undeformed. Lateral exposure of the Chuos Formation at this locality is limited, and thus descriptions on the macro- and micro-scale below will focus on upsection evolution of the deformation regime. For ease of description, the section has been divided into three structural zones,

shown on Fig 2. The lower and upper zones are dominated by ductile deformation structures (e.g. rotational features, dispersion tails, clast boudinage). The intermediate zone, meanwhile, is dominated by brittle deformation styles (e.g. fractured and crushed grains). Micromorphological terminology follows the style of Brewer (1976), as adapted by Menzies (2000), Zaniewski & van der Meer (2005) and Phillips et al. (2011) (see 8. Glossary).

4.1. Lower ductile zone (0-21 m)

4.1.1. Macroscale description

The basal 3 m of the Chuos Formation in Log 3 (Fig. 2) is characterised by massive to crudely laminated, poorly sorted diamictite. Evidence of deformation in this horizon is restricted to fractures traversing the larger outsized clasts (Fig. 3d). These sediments pass gradually upwards through moderately to well laminated diamictites. Approximately 14 m above the base of the section, these well laminated units exhibit asymmetric folds (Fig. 3e), clast attenuation and development of asymmetric pressure shadows. These features collectively record top-to-the-NW sense of simple shear.

At the south-eastern margin of the outcrop, these shear structures are overlain by a finely laminated siltstone (Fig. 3f), which coarsens upwards with the input of granule to small pebble sized clasts. The siltstone exhibits a concave-upward basal surface and planar upper surface, and pinches out laterally (to the NW), where no unconformity in the diamictite is visible. Above, the diamictite remains well laminated with deformation features including rotational turbate structures (Fig. 3g), clast dispersion tails and pervasive lineations on the clast surfaces, trending NNW (344°).

4.1.2. Microscale description

Micro-scale observations support a crudely developed lamination in the basal 3 m of the logged section, passing gradually upwards into more delicately laminated intervals (Fig. 4A). Rounded to sub-angular grains consist predominantly of quartzite, with minor feldspar, siltstone and clay intraclasts. Clast long axis orientations are variable, although a high proportion of grains exhibit a sub-horizontal microfabric (oriented N/NW to S/SE).

Planar features (e.g. linear grain alignments, symmetrical pressure shadows) are restricted to the base of this zone, whereas rotational deformation structures (e.g. turbate structures, dispersion tails, asymmetric pressure shadows and clast boudinage) are dominant throughout (Fig. 4A), and become progressively more abundant upsection. This is reflected in the development of necking structures between adjacent turbates (Fig. 5a). Bands of birefringent clay material (plasmic fabric) also become more distinct and pervasive upsection, varying from skel-masepic to skelsepic and unistrial. In places, this clay birefringence also outlines distinct S-C fabrics (Fig. 5e). These features, alongside the rotational structures, support a top-to-the N/NW shear sense. Towards the top of this zone, these structures and plasmic fabrics are cross-cut by sub-horizontal, non-birefringent clays, which in places demonstrate vertical, flame-like structures along their upper boundary.

4.2. Middle brittle zone

4.2.1. Macroscale description

At 21 m, poor exposure precludes detailed observation. At this interval, a metre thick unit of massive diamictite crops out, without evidence of macro-scale deformation.

4.2.2. Microscale description

The thin section is composed of poorly sorted, angular to sub-rounded quartz and feldspar grains which demonstrate no preferred orientation. Brittle deformation features, including

crushed quartz and fractured clasts, are common throughout, whereas ductile features were not observed. The abundant fracture surfaces can be correlated between adjacent grains across most of the section, resembling a 'jig-saw fit' pattern (Figs. 5 & 7e). A distinct birefringent fabric between the grains cannot be discerned.

4.3. Upper ductile zone

4.3.1. Macroscale description

Well laminated diamictite returns at 28 m, wherein a high proportion of clast long axes parallel the sub-horizontal lamination, and are in places attenuated along this fabric (Fig. 3h). Deformation is again dominated by rotational features including asymmetric boudins, S-C fabrics and turbate structures. This interval is cross-cut by a carbonate sedimentary dyke, consisting of brecciated fragments of the surrounding well laminated diamictite, set in a carbonate mudstone matrix (Fig. 3i).

4.3.2. Microscale description

This zone is characterised by a much smaller clast population than the underlying lower ductile and middle brittle zones, and becomes progressively more matrix-rich upsection accompanied by more distinct horizontal lamination (Fig. 4C). As in the lower ductile zone, rotational deformation features dominate, although conversely no planar features are present (e.g. linear grain alignments, symmetrical pressure shadows). Turbate structures and dispersion tails are abundant at the base of this zone, but diminish upsection where asymmetric pressure shadows and clast boudins are more prevalent (Fig. 5f-h). These features support a top-to-the NW sense of shear. Unistrial and skelsepic plasmic fabrics are highly developed throughout, as well as sub-horizontal clay-rich layers which parallel and cut

oblique to the plasmic fabric (Fig. 5f-h). As in the lower ductile zone, these clay layers exhibit flame structures along their upper boundary.

5. Discussion

5.1. Syn-sedimentary evolution of the Chuos Formation

Within the stratified diamictite facies, the widespread occurrence of outsized clasts with impact-related deformation structures (Fig. 3a) is interpreted as evidence of ice-rafted debris (IRD) (Thomas and Connell, 1985; Bennett et al., 1996; Condon et al., 2002), whereby derivation via sediment gravity flow rafting is rejected owing to the absence of characteristic clast imbrication, or correlation between bed thickness and maximum clast size (e.g. Martin et al, 1985; Postma et al., 1988). Water depths were sufficient to accumulate IRD at repeated stratigraphic intervals throughout deposition, but in the absence of diagnostic indicators, accumulation within a glaciomarine or glaciolacustrine basin cannot be ascertained. Large-scale cross-bed foresets within this facies (Log 2; Fig. 2) record tractive deposition and development of a simple barform, prograding towards the east. In view of the evidence favouring ice-rafting, these features are interpreted as ice-proximal subaqueous fan deposits (e.g. Powell & Domack, 1995; Powell, 2003; Hornung et al., 2007). The overlying soft-sediment striated surfaces (Fig. 3c), identical in morphology to those of the Hirnantian glacial record of North Africa (Sutcliffe et al., 2000; Le Heron et al., 2005), support the intrastratal transmission of shear stresses and subglacial deformation following subaqueous fan progradation. The absence of slickencrysts and polish on these surfaces discounts a later tectonic origin (Petit & Laville, 1987; Eyles & Boyce, 1998).

In the massive diamictite facies, glacial indicators are typically absent. This is considered to reflect glaciogenic debris flow remobilisation, consistent with the proposed ice-proximal

environment. In this setting, dynamic grounding-line oscillations would contribute to high rates of sediment supply, supported by the presence of subaqueous fan deposits and common coarsening upward profile of the diamictites (e.g. Benn, 1996; Evans et al., 2012), leading to rapid accumulation and oversteepening of the sediment pile. Resultant re-working of the glaciogenic sediments may also account, at least in part, for the unusual absence of striated and faceted clasts within the Chuos Formation.

In light of the location of the study area at the northern margin of an intracratonic fold belt (Miller, 2008), distinguishing the effects of soft-sediment or tectonogenetic deformation within the sheared and laminated diamictite facies remains paramount. Overall, the lack of bedding-discordant fabric development or metamorphic mineral overprint, and largely undeformed nature of the underlying and overlying formations indicate a soft-sediment genesis. In support, towards the top of Log 3 (Fig. 2) a carbonate dyke intrudes and brecciates the sheared diamictite (Fig. 3i), with evidence of liquefaction of clay and silt grade material along the intrusive contact. This is used to support a porewater-induced origin for the dyke, representing hydrofracturing of the sediment pile (e.g. van der Meer et al., 2009), and thus acts to support continued syn-sedimentary deformation *after* pervasive shearing and attenuation of the diamictite. Moreover, kinematic indicators throughout the section, all demonstrate top-to-the N/NW sense of shear (Figs. 3-5), consistent with the N-S strike of the grooves on the soft-sediment striated surfaces. Conversely, the dominant structural grain produced during Damaran orogenesis generated ENE-trending structures (Miller, 1983; Gray et al., 2008), cutting oblique to the trend of the sedimentary structures within the Chuos Formation.

5.2. Glacial vs. non-glacial deformation history

A striking feature of the described section, both on macro- and micro-scale, is the upsection increase in deformation intensity, reflected in the increased abundance and lateral attenuation of individual deformation structures. This incremental strain profile is a common feature within subglacial regimes (Boulton and Hindmarsh, 1987; Hart and Boulton, 1991; Benn and Evans, 1996; Evans et al., 2006; Hart, 2007), where the highest stress conditions are encountered at the ice-bed interface, towards the top of the bed, and diminish downwards. In contrast, deformation structures in a mass flow deposit exhibit the highest stress characteristics at base (see Fig. 6), where friction between the flow and the underlying substrate is greatest, thereby resulting in development of a basal shear zone accompanied by an upward decrease in strain intensity (Nardin et al., 1979; Nemec, 1990; Hart & Roberts, 1994; Mulder and Alexander, 2001).

Features considered diagnostic of sediment remobilisation, including flow noses and tile structures (Hart & Roberts, 1994; Bertran and Texier, 1999; Lachniet et al., 2001; Menzies & Zaniewski, 2003), are conspicuously absent from the Chuos Formation. The former are indicative of low shear, downslope slumping, and are hence rarely preserved under high stress subglacial deformation (Lowe, 1982; Hart & Roberts, 1994), whilst the latter appear to be a unique feature associated with deceleration and dewatering of sediment gravity flows (Menzies & Zaniewski, 2003; van der Meer & Menzies, 2011). Similarly, clasts with coatings of diamictite on the macro-scale, or concentrically laminated grain coatings on the micro-scale, though not diagnostic, would support sediment re-working if present (Phillips, 2006; Kilfeather et al., 2009). Furthermore, the absence of load structures and rare evidence of vertical to sub-vertical water escape structures may be considered atypical of mass flow

deposition (Lowe, 1982; Visser et al., 1984; Hart & Roberts, 1994; Menzies & Zaniewski, 2003).

Rotational deformation structures are ubiquitous in the Chuos Formation, particularly on the micro-scale (Figs. 4-5), and are encountered in both subglacial settings and sediment gravity flows (Lachniet et al., 2001; Menzies and Zaniewski, 2003; Phillips, 2006). In the former, these features are interpreted as the product of shearing within the deforming bed (van der Meer, 1993, 1997), whereby stress is accommodated around a rotating nucleus (consisting of a core stone or stiff matrix), leading to preferential alignment of smaller clasts at the nucleus periphery. Similar mechanisms are envisaged in sediment gravity flows, although rotation acts as a product of transient turbulent cells within the depositing flow (Phillips, 2006).

Although the latter mechanism cannot be excluded, the absence of other features indicative of turbulence (e.g. normally graded beds), as compared to abundant evidence of pervasive shearing, is compatible with a glaciectonic origin for the turbates. This is also supported by their association with planar shear fabrics and structures throughout (cf. Hiemstra & Rijdsdijk, 2003).

Additional deformation structures frequently cited as evidence of subglacial processes are prevalent throughout (see Fig. 6), including pervasive tectonic lamination, unidirectional folding, pressure shadows and clast dispersion tails (e.g. van der Meer, 1993; Hart & Roberts, 1994; Benn & Evans, 1996; Menzies et al., 1997; Lachniet et al. 2001; Carr et al., 2006; Menzies et al., 2006). These features support ductile deformation under high cumulative stress, facilitated by elevated porewater pressures, which succeed in lowering the effective stress of the sediment (Menzies, 2000; Phillips et al., 2007; Lee & Phillips, 2008). These conditions are commonly encountered in subglacial settings under the high overburden pressure of ice and abundant basal meltwater supply (see section 5.3). This is also supported

by the presence of fractured and crushed grains, which frequently develop in zones of high hydrostatic pressure near the ice-bed interface (Hiemstra and van der Meer, 1997; Menzies, 2000; Carr et al., 2006).

5.3. Hydrology of the subglacial bed

In view of the sedimentological evidence of primary deposition as a subaqueous diamictite, it would be plausible to consider the sediments as water-saturated, and thus with elevated porewater contents, prior to subglacial deformation. Nonetheless, the observed upsection increase in strain intensity, alongside attenuation and lateral isolation of individual microstructures, reflects sustained and increasing high porewater pressures throughout deformation.

In a subglacial environment, the effect of overriding ice on porewater state will be threefold: 1) overburden pressure will increase confining pressure on the deforming bed, 2) the ice will act as an impermeable seal inhibiting vertical water escape, and 3) friction at the ice-bed interface will generate abundant basal meltwater, thereby increasing porewater content (Evans and Hiemstra, 2005; Phillips et al., 2007; Lee & Phillips, 2008, 2011). A common process in this scenario will be the development of lateral water escape features (Roberts and Hart, 2005; Lee & Phillips, 2008), in this succession generating abundant sub-horizontal clay –filled conduits. These features, in conjunction with well developed plasmic fabrics throughout, support high concentrations of impermeable clay minerals within the sediment, which act to further retard water escape from the deforming bed (Denis et al., 2009; Lesemann et al. 2010). These factors will thus enable increased dilation of the sediment, whereby the zone of subglacial shearing can extend deeper within the deforming sediment pile (Lee & Phillips, 2008).

328 If porewater pressures continue to rise, stress at the ice-bed interface will reach critical levels
 329 enabling the ice to decouple from its substrate (Evans et al., 2006), especially in contact with
 330 underlying bed irregularities. This will typically result in infill of fine grained sediments
 331 within the subglacial cavity, preserved as discontinuous lens-shaped beds (Evans & Benn,
 332 2004; Lesemann et al., 2010). This interpretation is favoured for the finely laminated siltstone
 333 recorded at the south-eastern margin of Log 3 (Fig. 3f). In contrast, when porewater pressures
 334 are reduced, e.g. in response to enhanced water escape or freezing of the subglacial bed,
 335 porewater influenced deformation will be inhibited, potentially leading to ‘locking-up’ of the
 336 deforming material (Evans et al., 2006; Lee & Phillips, 2008). As a result, the previously
 337 water-saturated sediment may undergo brittle brecciation, as recorded in the middle brittle
 338 zone (Fig. 4B). The jig-saw fit pattern of adjacent fractured surfaces (Fig. 5c) supports *in situ*
 339 brecciation of this unit, consistent with rapid de-watering and deceleration of the mobile
 340 deforming bed. This de-watering horizon in the middle of the sequence may therefore be used
 341 to distinguish at least two phases of increasing porewater pressure during deformation of the
 342 Chuos Formation, in-keeping with the characteristic polyphase nature of subglacial
 343 deformation regimes (e.g. van der Meer, 1993; Menzies, 2000; Phillips et al., 2007, 2008).

344 5.4. Ice marginal model for the deposition and deformation of the Chuos Formation

345 Recent studies of stratified glacial diamictites within ice marginal environments have
 346 advocated accumulation of thick, variably deformed sediment piles through the combined
 347 effects of high sediment supply and glaciotectonic thrusting (e.g. Evans & Hiemstra, 2005; Ó
 348 Cofaigh et al., 2011; Evans et al. 2012). In these settings, pre-existing stratification within the
 349 sediment, commonly produced in response to the heterogeneous sediment inputs encountered
 350 at the ice margin, encourages deformation partitioning along bed surfaces. Repeated
 351 oscillations of the ice margin will therefore exploit these pre-existing structural weaknesses,

352 leading to glaciotectonic thrusting and stacking, and hence incremental thickening of the
 353 succession. Depending on the extent of ice advance, these oscillations can also lead to
 354 overriding of the sediment pile (Ó'Cofaigh et al., 2011), resulting in subglacial as well as ice
 355 marginal deformation.

356 A similar setting is envisaged to account for the sedimentological and structural features
 357 preserved within the Chuos Formation. The development of sub-horizontal lamination at the
 358 relatively less deformed base of Log 3 (Fig. 2), alongside the widespread occurrence of
 359 stratified diamictites throughout the Chuos Formation, support the generation of a syn-
 360 depositional, or 'pre-existing' stratification. Subsequent deformation of the sediment pile
 361 clearly resulted in deformation partitioning along bed/lamina contacts since tectonic
 362 lamination, shear structures and plasmic fabrics are bed-parallel throughout. However, in
 363 contrast to previous studies (e.g. Evans & Hiemstra, 2005; O'Cofaigh et al. 2011; Evans et al.
 364 2012) a significant thrust component was not recorded in the Chuos Formation. It is possible
 365 that sub-horizontal shear surfaces within the sediment also operated as thrust planes during
 366 proglacial to submarginal deformation, leading to progressive stacking and thickening of the
 367 sediment pile. Alternatively, in light of the evidence for high porewater contents and
 368 significant ice overburden pressure, vertical stacking of the deforming bed may not have been
 369 possible, resulting in lateral attenuation and 'smearing' of the sediment pile as opposed to
 370 thrust-related aggradation. This may also reflect the subglacial position of the sediment
 371 throughout deformation, where it would have been sheltered from proglacial and ice marginal
 372 tectonics. In contrast, discrete bed-scale horizons of subglacial deformation associated with
 373 the grounding-line fan deposits (Log 2; Fig. 2) likely reflect periodic overriding in ice
 374 marginal positions, with potentially thrust-related shearing accommodated in the soft-
 375 sediment striated surfaces (Fig. 3c).

6. Conclusions

The Chuos Formation in the Otavi Mountainland, northern Namibia, accumulated in an ice-proximal subaqueous environment prior to secondary subglacial deformation. Detailed analysis of soft sediment deformation structures was critical in determining the presence and influence of grounded ice at this time. These features, in conjunction with the deposition of ice-proximal subaqueous fan deposits, and abundant ice-rafted debris at recurrent stratigraphic intervals throughout the Chuos diamictites act to support dynamic oscillations of the ice grounding-line. Therefore, the unusual paucity of ‘classic’ glacial indicators (i.e. striated and facteted clasts, striated pavements) does not preclude Neoproterozoic glaciation, as frequently argued under sediment gravity follow hypotheses. Soft sediment deformation structures are thus considered as key, and largely under-considered, palaeoclimate proxies, with significant implications for determining the glaciogenic origin of pan-global diamictite successions, as well as the nature of subglacial bed conditions during the Neoproterozoic icehouse.

7. Acknowledgments

The authors wish to thank Paulus N. Mungandjera and Ralph J.C.M. Muyamba, UNAM, for their invaluable field assistance, and the owners of Ghaub and Varianto Farms for granting permission to examine these sections on their land. Thanks also to Kevin D’Souza, RHUL, for assistance with thin section photography.

8. Glossary

Based on Brewer (1976), as adapted by Menzies (2000), and Zaniewski and van der Meer (2005,) unless otherwise stated.

Dispersion tail: concentration of smaller grains or plasma in the lee of a larger grain.

Necking structure: variety of turbate structure. Alignment of smaller grains occurs between adjacent larger grains (Lachniet et al. 1999).

Plasma: particles of colloidal size ($<20\text{ }\mu\text{m}$), including mineral and organic material, within which individual grains cannot be discerned.

Plasmic fabric: orientation of plasma domains based on the optical properties (birefringence) of aligned plasma particles. Common varieties include:

Asepic: anisotropic plasma domains with little to no preferred orientation. Sub-varieties include Argillasepic (dominantly clay-sized particles) and Silasepic (dominantly silt-sized particles).

Masepic: short plasmic fabric domains with a single preferred orientation.

Bimasepic: plasma particles exhibit two dominant preferred orientations. Termed *Lattisepic* where these directions are perpendicular.

Insepic: small clusters of oriented plasma particles where clusters show no preferred orientation.

Multisepic: multiple (>2) preferred plasmic fabric orientations.

Skelsepic: plasmic particles preferentially oriented around skeleton grains.

Omnisepic: random orientation of various plasmic fabric domains.

Unistrial: elongate, discrete bands of birefringent clay plasma.

Pressure shadow: Typically massive domain of lower strain adjacent to a clast. Synonymous with strain shadow (Phillips et al. 2011).

Turbate structure: circular arrangement of grains around a core stone or stiff matrix. Long axes of oriented grains exhibit a parallel or radial orientation relative to the margins of the core stone (Hiemstra & Rijsdijk, 2003).

9. References

- Allen, P.A., Etienne, J.L., 2008. Sedimentary challenge to Snowball Earth. *Nature Geoscience*, 1, 817-825.
- Arnaud, E., 2008. Deformation in the Neoproterozoic Smalfjord Formation, northern Norway: an indicator of glacial depositional conditions? *Sedimentology*, 55, 335-356.
- Arnaud, E., 2012. The paleoclimatic significance of deformation structures in Neoproterozoic successions. *Sedimentary Geology*, 243-244, 33-56.
- Benn, D.I., 1996. Subglacial and subaqueous processes near a glacier grounding line: Sedimentological evidence from a former ice-dammed lake, Achnasheen Scotland. *Boreas*, 25, 23-36.
- Benn, D.I., Evans, D.J.A., 1996. The interpretation and classification of subglacially-deformed materials. *Quaternary Science Reviews*, 15, 23-52.
- Benn, D.I., Prave, A.R., 2006. Subglacial and proglacial glacitectonic deformation in the Neoproterozoic Port Askaig Formation, Scotland. *Geomorphology*, 75, 266-280.
- Bennett, M.R., Doyle, P., Mather, A.E., 1996. Dropstones: Their origin and significance. *Palaeogeography, Palaeoclimatology, Palaeoecology*, 121, 331-339.
- Bertran, P., Texier, J.-P., 1999. Facies and microfacies of slope deposits. *Catena*, 35, 99-121.
- Boulton, G.S., Hindmarsh, R.C.A., 1987. Sediment Deformation beneath Glaciers - Rheology and Geological Consequences. *Journal of Geophysical Research-Solid*, 92, 9059-9082.
- Brewer, R. 1976. *Fabric and Mineral Analysis of Soils*. Krieger, Huntington, 482 p.
- Carr, S.J. 2004. Micro-scale features and structures. In: Evans, D.J.A., Benn, D.I. (eds.) *A practical guide to the study of glacial sediments*. Arnold, New York, p. 115-144.
- Carr, S.J., Holmes, R., van der Meer, J.J.M., Rose, J., 2006. The Last Glacial Maximum in the North Sea Basin: micromorphological evidence of extensive glaciation. *Journal of Quaternary Science*, 21, 131-153.
- Condon, D.J., Prave, A.R., Benn, D.I., 2002. Neoproterozoic glacial-rainout intervals: Observations and implications. *Geology*, 30, 35-38.

- Denis, M., Guiraud, M., Konaté, M., Buoncristiani, J.F., 2009. Subglacial deformation and water-pressure cycles as a key for understanding ice stream dynamics: evidence from the Late Ordovician succession of the Djado Basin (Niger). *International Journal of Earth Sciences*, 99, 1399-1425.
- Etienne, J.L., Allen, P.A., Rieu, R., Le Guerroué, E. 2007. Neoproterozoic Glaciated Basins: A critical review of the Snowball Earth hypothesis by comparison with Phanerozoic Glaciations. In: Hambrey, M.J., Christoffersen, P., Glasser, N.F., Hubbard, B. *Glacial Sedimentary Processes and Products*. Blackwell Publishing Ltd, Oxford, p. 343-399.
- Evans, D.J.A. and Benn, D.I. (2004) *A Practical Guide to the Study of Glacial Sediments*. Arnold, New York. 266 pp.
- Evans, D.J.A., Hiemstra, J.F., 2005. Till deposition by glacier submarginal, incremental thickening. *Earth Surface Processes and Landforms*, 30, 1633-1662.
- Evans, D.J.A., Hiemstra, J.F., Cofaigh, C.Ó., 2012. Stratigraphic architecture and sedimentology of a Late Pleistocene subaqueous moraine complex, southwest Ireland. *Journal of Quaternary Science*, 27, 51-63.
- Evans, D.J.A., Phillips, E.R., Hiemstra, J.F., Auton, C.A., 2006. Subglacial till: Formation, sedimentary characteristics and classification. *Earth Science Reviews*, 78, 115-176.
- Eyles, N., Boyce, J.I., 1998. Kinematic indicators in fault gouge: tectonic analog for soft bedded ice sheets. *Sedimentary Geology*, 116, 1 – 12.
- Eyles, N., Januszczak, N., 2004. ‘Zipper-rift’: a tectonic model for Neoproterozoic glaciations during the breakup of Rodinia after 750 Ma. *Earth Science Reviews*, 65, 1-73.
- Eyles, N., Januszczak, N., 2007. Syntectonic subaqueous mass flows of the Neoproterozoic Otavi Group, Namibia: where is the evidence of global glaciation? *Basin Research*, 19, 179-198.
- Geological Survey of Namibia, 2008. Sheet 1916- Tsumeb (1:250,000). Ministry of mines and Energy, Windhoek.
- Gevers, T.W., 1931. An ancient tillite in South-West Africa. *Transactions of the Geological Society of South Africa*, 34, 1-17.
- Gray, D.R., Foster, D.A., Meert, J.G., Goscombe, R. et al. 2008. A Damara orogen perspective on the assembly of southwestern Gondwana. Geological Society, London, Special Publications, 294, 257-278.
- Hart, J.K., 2007. An investigation of subglacial shear zone processes from Weybourne, Norfolk, UK. *Quaternary Science Reviews*, 26, 2354-2374.
- Hart, J.K., Boulton, G.S., 1991. The interrelation of glaciotectonic and glaciodepositional processes within the glacial environment. *Quaternary Science Reviews*, 10, 335-350.

- 486 Hart, J.K., Roberts, D.H., 1994. Criteria to Distinguish between Subglacial Glaciotectonic
487 and Glaciomarine Sedimentation .1. Deformation Styles and Sedimentology.
488 Sedimentary Geology, 91, 191-213.
- 489 Hedberg, R.M. 1979. Stratigraphy of the Ovamboland Basin, South West Africa Bulletin.
490 Precambrian Research Unit, Cape Town, 325 pp.
- 491 Henry, G., Stanistreet, I.G., Maiden, K.J., 1986. Preliminary results of a sedimentological
492 study of the Chuos Formation in the central zone of the Damara Orogen: evidence for
493 mass flow processes and glacial activity. Communications of the Geological Survey
494 of South-West Africa/ Namibia, 2, 75-92.
- 495 Hiemstra, J.F., Rijsdijk, K.F., 2003. Observing artificially induced strain: implications for
496 subglacial deformation. Journal of Quaternary Science, 18, 373-383.
- 497 Hiemstra, J.F., van der Meer, J.J.M., 1997. Pore-water controlled grain fracturing as an
498 indicator for subglacial shearing in tills. Journal of Glaciology, 43, 446-454.
- 499 Hoffman, P.F., Hawkins, D.P., Isachsen, C.E., and Bowring, S.A., 1996, Precise U-Pb zircon
500 ages for early Damaran magmatism in the Summas Mountains and Welwitschia Inlier,
501 northern Damara belt, Namibia: Communications of the Geological Survey of
502 Namibia, v. 11, p. 47-52.
- 503 Hoffman, P.F., Kaufman, A.J., Halverson, G.P., Schrag, D.P., 1998. A Neoproterozoic
504 snowball earth. Science, 281, 1342-1346.
- 505 Hoffman, P.F., Schrag, D.P., 2002. The snowball Earth hypothesis: testing the limits of
506 global change. Terra Nova, 14, 129-155.
- 507 Hoffman, P.F., Halverson, G.P., 2008. Otavi Group of the western Northern Platform, the
508 eastern Kaoko Zone and the western Northern Margin Zone. In Miller, R. McG.
509 (Ed.), The Geology of Namibia. Volume 2: Neoproterozoic to Lower Palaeozoic.
510 Ministry of Mines and Energy, pp. 13.69- 13-136.
- 511 Hoffmann, K-H. 1983. Lithostratigraphy and facies of the Swakop Group of the southern
512 Damara Belt, SWA/Namibia. In: Miller, R. McG. (ed.) Evolution of the Damara
513 Orogen of southwest Africa/Namibia. Geological Society of South Africa Special
514 Publication, 11, 43-63.
- 515 Hoffmann, K-H., Prave, A.R., 1996. A preliminary note on a revised subdivision and regional
516 correlation of the Otavi Group based on glaciogenic diamictites and associated cap
517 dolostones. Communications of the Geological Survey of Namibia, 11, 77-82.
- 518 Hoffmann, K.H., Condon, D.J., Bowring, S.A., Crowley, J.L., 2004. U-Pb zircon date from
519 the Neoproterozoic Ghaub Formation, Namibia: Constraints on Marinoan glaciation.
520 Geology, 32, 817-820.

- Hornung, J.J., Asprion, U., Winsemann, J., 2007. Jet-efflux deposits of a subaqueous ice-contact fan, glacial Lake Rinteln, northwestern Germany. *Sedimentary Geology*, 193, 167-192.
- Kennedy, M.J., Runnegar, B., Prave, A.R., Hoffmann, K.H., Arthur, M.A., 1998. Two or four Neoproterozoic glaciations? *Geology*, 26, 1059-1063.
- Kilfeather, A.A., Ó Cofaigh, C., Dowdeswell, J.A., Meer, J.J.M., Evans, D.J.A., 2009. Micromorphological characteristics of glacial marine sediments: implications for distinguishing genetic processes of massive diamicts. *Geo-Marine Letters*, 30, 77-97.
- Kirschvink, J.L., 1992, Late Proterozoic low-latitude glaciation: the snowball Earth. In: Schopf, J.W. & Klein, C. (eds.) *The Proterozoic Biosphere*. Cambridge University Press, Cambridge, p. 51-52.
- Kroner, A., Rankama, K. 1973. Late Precambrian glaciogenic sedimentary rocks in southern Africa: a compilation with definitions and correlations. *Bulletin of the Geological Society of Finland*, 45, 79-102.
- Lachniet, M.S., Larson, G.J., Lawson, D.E., Evenson, E.B., Alley, R.B., 2001. Microstructures of sediment flow deposits and subglacial sediments: a comparison. *Boreas*, 30, 254-264.
- Lee, J.R., Phillips, E.R., 2008. Progressive soft sediment deformation within a subglacial shear zone—a hybrid mosaic—pervasive deformation model for Middle Pleistocene glaciotectionised sediments from eastern England. *Quaternary Science Reviews*, 27, 1350-1362.
- Lee, J.R., Phillips, E. 2011. Development of a ‘soft deforming bed’ within a subglacial shear zone: an example from Bacton Green. In: Phillips, E., Lee, J.R., Evans, H.M. (eds.) *Glacitectonics – Field Guide*. Quaternary Research Association, UK, p. 130-142.
- Le Heron, D.P., Sutcliffe, O.E., Whittington, R.J. and Craig, J. (2005) The origins of glacially related soft-sediment deformation structures in Upper Ordovician glaciogenic rocks: implication for ice sheet dynamics. *Palaeogeography, Palaeoclimatology, Palaeoecology*, 218, 75–103.
- Lesemann, J.-E., Alsop, G.I., Piotrowski, J.A., 2010. Incremental subglacial meltwater sediment deposition and deformation associated with repeated ice-bed decoupling: a case study from the Island of Funen, Denmark. *Quaternary Science Reviews*, 29, 3212-3229.
- Lowe, D.R. (1982) Sediment gravity flows: II. Depositional models with special reference to the deposits of high-density turbidity currents. *Journal of Sedimentary Petrology*, 52, 279-297.
- Martin, H. 1965a. Beobachtungen zum problem der jung-präkambrischen glazialen Ablagerungen in Südwesafrika. *Geologische Rundschau*, 54, p. 115.

- 558 Martin, H. 1965b. The Precambrian geology of South West Africa and Namaqualand.
559 Precambrian Research Unit, University of Cape Town.
- 560 Martin, H., Porada, H., Walliser, O.H., 1985. Mixtite Deposits of the Damara Sequence,
561 Namibia, Problems of Interpretation. *Palaeogeography, Palaeoclimatology,*
562 *Palaeoecology*, 51, 159-196.
- 563 Menzies, J. 2000. Micromorphological analyses of microfabrics and microstructures indicative
564 of deformation processes in glacial sediments. In: Maltman, A.J., Hubbard, B.,
565 Hambrey, M.J. (eds.) *Deformation of Glacial Materials*. Geological Society Special
566 Publication No. 176, London, p. 245-257.
- 567 Menzies, J., van der Meer, J.J.M., Rose, J., 2006. Till—as a glacial “tectonict”, its internal
568 architecture, and the development of a “typing” method for till differentiation.
569 *Geomorphology*, 75, 172-200.
- 570 Menzies, J., Zaniewski, K., 2003. Microstructures within a modern debris flow deposit
571 derived from Quaternary glacial diamicton—a comparative micromorphological
572 study. *Sedimentary Geology*, 157, 31-48.
- 573 Menzies, J., Zaniewski, K., Dreger, D., 1997. Evidence, from microstructures, of deformable
574 bed conditions within drumlins, Chimney bluffs, New York State. *Sedimentary*
575 *Geology*, 111, 161-175.
- 576 Miller, R. McG. 1983. Tectonic implications of the contrasting geochemistry of Damaran
577 mafic volcanic rocks, South West Africa/Namibia. In: Miller, R. McG. (ed.)
578 *Geodynamic evolution of the Damara Orogen*. Geological Society of South Africa
579 Special Publication, 115-138.
- 580 Miller, R. McG. (Ed.). 2008. *The Geology of Namibia. Volume 2: Neoproterozoic to Lower*
581 *Palaeozoic*. Ministry of Mines and Energy.
- 582 Mulder, T., Alexander, J., 2001. The physical character of subaqueous sedimentary density
583 flows and their deposits. *Sedimentology*, 48, 269-299.
- 584 Nardin, T.R., Hein, F.J., Gorsline, D.S. and Edwards, B.D. (1979) A review of mass
585 movement processes, sediment and acoustic characteristics and contrasts in slope and
586 base of slope systems versus canyon-fan basin floor systems. In: *Geology of*
587 *Continental Slopes* (Eds. L.J. Doyle, O.H. Pilkey), SEPM Special Publication, 61–73.
- 588 Nemec, W. 1990. Aspects of sediment movement on steep delta slopes. In: Colella, A., Prior,
589 D. (eds.) *Coarse Grained Deltas*. International Association of Sedimentologists,
590 Special Publication, 10, 29-73.
- 591 Ó Cofaigh, C., Evans, D.J.A., Hiemstra, J.F., 2011. Formation of a stratified subglacial ‘till’
592 assemblage by ice-marginal thrusting and glacier overriding. *Boreas*, 40, 1-14.
- 593 Petit, J.-P., Laville, E., 1987. Morphology and microstructures of hydroplastic slickensides in
594 sandstone. In: Jones, M.E., Preston, R.M.F. (Eds.), *Deformation of Sediments and*

- Sedimentary Rocks. Geological Society of London Special Publication, vol. 29, pp. 107–121.
- Phillips, E., 2006. Micromorphology of a debris flow deposit: evidence of basal shearing, hydrofracturing, liquefaction and rotational deformation during emplacement. *Quaternary Science Reviews*, 25, 720-738.
- Phillips, E., Lee, J.R., Burke, H. 2008. Progressive proglacial to subglacial deformation and syntectonic sedimentation at the margins of the Mid-Pleistocene British Ice Sheet: evidence from north Norfolk, UK. *Quaternary Science Reviews*, 27, 19-20.
- Phillips, E., Merritt, J., Auton, C., Golledge, N., 2007. Microstructures in subglacial and proglacial sediments: understanding faults, folds and fabrics, and the influence of water on the style of deformation. *Quaternary Science Reviews*, 26, 1499-1528.
- Phillips, E., van der Meer, J.J.M., Ferguson, A. 2011. A new 'microstructural mapping' methodology for the identification, analysis and interpretation of polyphase deformation within subglacial sediments. *Quaternary Science Reviews*, 30, 2570-2596.
- Porada, H. 1983. Geodynamic model for the geosynclinal development of the Damara Orogen, Namibia, South West Africa. In: Martin, H., Eder, F.W. (eds.) *Intracontinental Fold Belts – Case studies in the Variscan Belt of Europe and the Damara Belt in Namibia*. Springer, Heidelberg, pp. 503-540.
- Porada, H., Wittig, R. 1983a. Turbidites in the Damara Orogen. In: Martin, H., Eder, F.W. (eds.) *Intracontinental Fold Belts – Case studies in the Variscan Belt of Europe and the Damara Belt in Namibia*. Springer, Heidelberg, pp. 543-576.
- Porada, H., Wittig, R. 1983b. Turbidites and their significance for the geosynclinal evolutions of the Damara Orogen, South West Africa, Namibia. In: Miller, R. McG. (ed.) *Geodynamic evolution of the Damara Orogen*. Geological Society of South Africa Special Publication, 115-138.
- Postma, G., Nemec, W., Kleinspehn, K.L., 1988. Large Floating Clasts in Turbidites - a Mechanism for Their Emplacement. *Sedimentary Geology*, 58, 47-61.
- Powell, R.D. 2003. Subaquatic landsystems: fjords. In: Evans, D.J.A. (ed.) *Glacial Landsystems*. Arnold, London, 313-347.
- Powell, R., Domack, E. 1995. Modern glaciomarine environments. In: Menzies, J. (ed.) *Modern Glaciomarine Environments – Processes, Dynamics and Sediments*, Vol. 1. Butterworth-Heinemann, Oxford, 445-486.
- Roberts, D.H., Hart, J.K., 2005. The deforming bed characteristics of a stratified till assemblage in north East Anglia, UK: investigating controls on sediment rheology and strain signatures. *Quaternary Science Reviews*, 24, 123-140.

- Shields, G.A., 2005. Neoproterozoic cap carbonates: a critical appraisal of existing models and the plumeworld hypothesis. *Terra Nova*, 17, 299-310.
- Sutcliffe, O.E., Theron, J.A., Whittington, R.J., Theron, J.N., Craig, J., 2000. Calibrating the Late Ordovician glaciation and mass extinction by the eccentricity cycles of the Earth's orbit. *Geology*, 23, 967-970.
- Thomas, G.S.P., Connell, R.J., 1985. Iceberg Drop, Dump, and Grounding Structures from Pleistocene Glacio-Lacustrine Sediments, Scotland. *Journal of Sedimentary Petrology*, 55, 243-249.
- van der Meer, J.J.M. 1987. Micromorphology of glacial sediments as a tool in distinguishing genetic varieties of till. *Geological Survey of Finland, Special Paper*, 3, p. 77-89.
- van der Meer, J.J.M. 1993. Microscopic evidence of subglacial deformation. *Quaternary Science Reviews*, 12, 553-587.
- van der Meer, J.J.M. 1997. Subglacial processes revealed by the microscope: particle and aggregate mobility in till. *Quaternary Science Reviews*, 16, 827-831.
- van der Meer, J.J.M., Kjær, K.H., Krüger, J., Rabassa, J., Kilfeather, A.A., 2009. Under pressure: clastic dykes in glacial settings. *Quaternary Science Reviews*, 28, 708-720.
- van der Meer, J.J.M., Menzies, J., 2011. The micromorphology of unconsolidated sediments. *Sedimentary Geology*, 238, 213-232.
- Visser, J.N.J., Colliston, W.P., Terblanche, J.C. 1984. The origin of soft sediment deformation structures in Permo-Carboniferous glacial and proglacial beds, South Africa. *Journal of Sedimentary Petrology*, 54, 1183-1196.
- Zaniewski, K., van der Meer, J.J.M. 2005. Quantification of plasmic fabric through image analysis. *Catena*, 63, 109-127.

Figure captions

Figure 1: A. Map outlines stratigraphic framework of Namibia, and the location of the study sites in the Otavi Mountainland, along the south-eastern flank of the Owambo Basin, after Miller (2008). B. Stratigraphy of the Cryogenian succession exposed in the study area, after Hoffman & Prave (1996).

Figure 2: Logged sections of the Chuos Formation, located on inset geological map of Ghaub and Varianto Farm study areas. Note the overall lateral transition from massive to stratified diamictites towards the west/north-west. The stratigraphic location of images shown in figures 3-5 are indicated by their corresponding numbers adjacent to the logs. Map modified after Geological Survey of Namibia (2008).

Figure 3: Macro-scale sedimentary and deformation structures. Coin and lens cap for scale measure 2 cm and 5 cm, respectively. A) Outsized clast with impact-related deformation structure, indicated by white arrows. B) Fractured clast infilled by diamictite. C) North-south trending linear grooves and ridges interpreted as soft-sediment striated surfaces. D) Fractured outsized clast within the comparatively undeformed base of Log 3 (Fig. 2). E) Asymmetric fold demonstrating top-to-the-NW vergence. Note clast attenuation parallel to deformed laminae. F) Laminated siltstone lens, interpreted as ice-bed separation feature, restricted to the south-eastern margin of the exposed section (Log 3; Fig. 2). G) Rotational turbate structure showing preferential alignment of smaller clasts around the margins of the central obstacle clast (picked out by white dashed lines). Note top-to-the-SE shearing and abrasion of core stone. H) Pervasive tectonic lamination. Asymmetric clast boudinage and S-C structures define a top-to-the-NW shear sense. I) Carbonate dyke cross-cuts sheared diamictite (G). Note brecciated fragments of deformed diamictite within the dyke.

Figure 4: Paired thin section photograph and interpretation of Chuos Formation microstructures. *Lower Ductile Zone:* A) Well developed sub-horizontal fabric and abundant rotational deformation structures (turbate structures, asymmetric boudins, clast dispersion tails and asymmetric pressure shadows). Microstructures support top-to-the-NW shear sense. *Middle Brittle Zone:* B) This sample is characterised by fractured and crushed quartz grains (white) and magnetite crystals (black). Fractured surfaces can be traced between adjacent clasts, akin to a ‘jig-saw’ pattern, indicating *in situ* clast breakage. Sense of deformation cannot be ascertained. *Upper Ductile Zone:* C) Microstructures are highly attenuated, defined

by the predominance of sheared clast boudins. These features, alongside asymmetrical pressure shadows and rare rotational turbates support top-to-the-NW deformation. Note sub-horizontal clay layers cutting oblique to tectonic lamination, with flame-like structures on their upper boundary.

Figure 5: Micro-scale deformation structures. Photos A-D captured under plane-polarized light, E-H under cross-polarized light. White bar for scale measures 1 mm. Lower Ductile Zone: A) Necking structure developed between adjacent turbate structures. B) Central rotational deformation structure with associated ‘tails’ of silt-grade sediment and small sand clasts. Top-to-the-NW shear sense also supported by asymmetric pressure shadow in the uppermost portion of the image. Middle Brittle Zone: C) Dashed lines highlight ‘jig-saw fit’ fractured grain surfaces. Upper Ductile Zone: D) Rotational structure with fabric-parallel ‘tails’ of clay-grade sediment and small sand grains. Abrasion and fracturing of core stone interpreted as product of pervasive shearing. E) Birefringent clay particles outline S-C fabrics, supporting top-to-the-N shear sense. F) Asymmetric pressure shadow outlined by skelsepic-unistrial plasmic fabric. Note discontinuous clay layers trending both parallel and oblique to the plasmic fabric (black arrow). G-H) Well developed unistrial to skelsepic plasmic fabric surrounding boudinaged skeleton grains. Note discontinuous clay layers cutting oblique to the plasmic fabric (black arrow).

Figure 6: Schematic diagram highlights dominant style and association of deformation structures typically encountered within a sediment gravity flow as compared to the assemblage identified in the Chuos Formation. Length of black arrow corresponds to strain intensity, wherein the former would be expected to demonstrate a basal shear zone with upward decreasing strain intensity, vertical water-escape structures and abundant evidence of re-working (e.g. diamictite intraclasts, laminated clast coatings, slump folds). In contrast, the observed upsection increase in strain intensity, abundance of ductile deformation features, pervasive tectonic lamination, and sub-horizontal water-escape features act to support subglacial deformation under high cumulative stress and elevated porewater pressures. Adapted after Evans et al. (2012) and Phillips (2006).

Figure 7: Ice marginal model for the deposition and subsequent deformation of the Chuos Formation. Ice-proximal subaqueous deposition occurs through the combined input of ice-rafted, englacial, supraglacial and subglacial debris, building out as ice-contact subaqueous

725 fans. During grounding-line oscillations, these sediments undergo subglacial deformation
1
2 726 processes behind the ice front, periodic mass wasting in advance of the ice front, as well as
3
4 727 proglacial to ice marginal intrastratal shear. Modified after Ó'Cofaigh et al. (2011) and Evans
5
6 728 et al. (2012).
7
8
9
10
11
12
13
14
15
16
17
18
19
20
21
22
23
24
25
26
27
28
29
30
31
32
33
34
35
36
37
38
39
40
41
42
43
44
45
46
47
48
49
50
51
52
53
54
55
56
57
58
59
60
61
62
63
64
65

Figure

[Click here to download high resolution image](#)

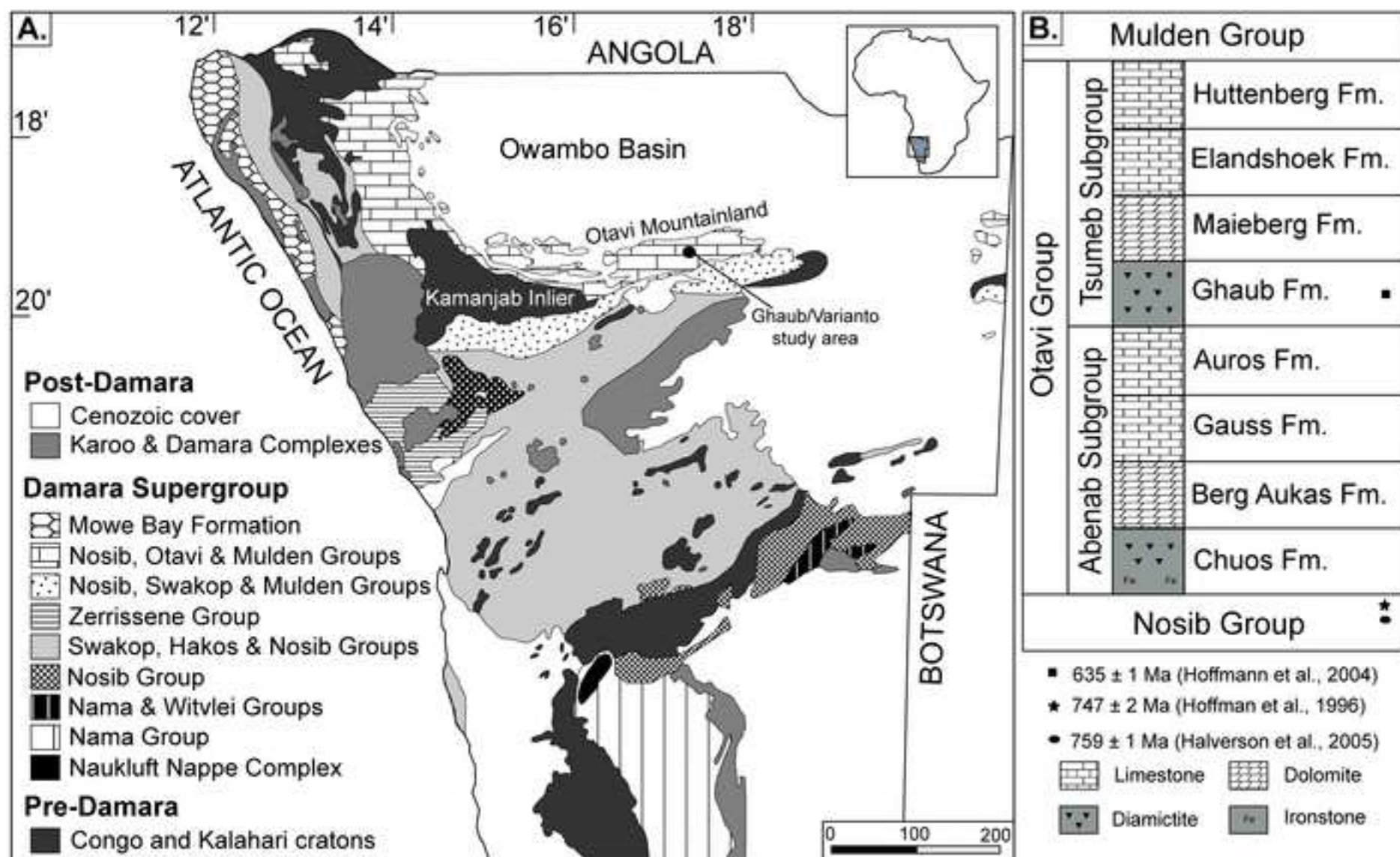
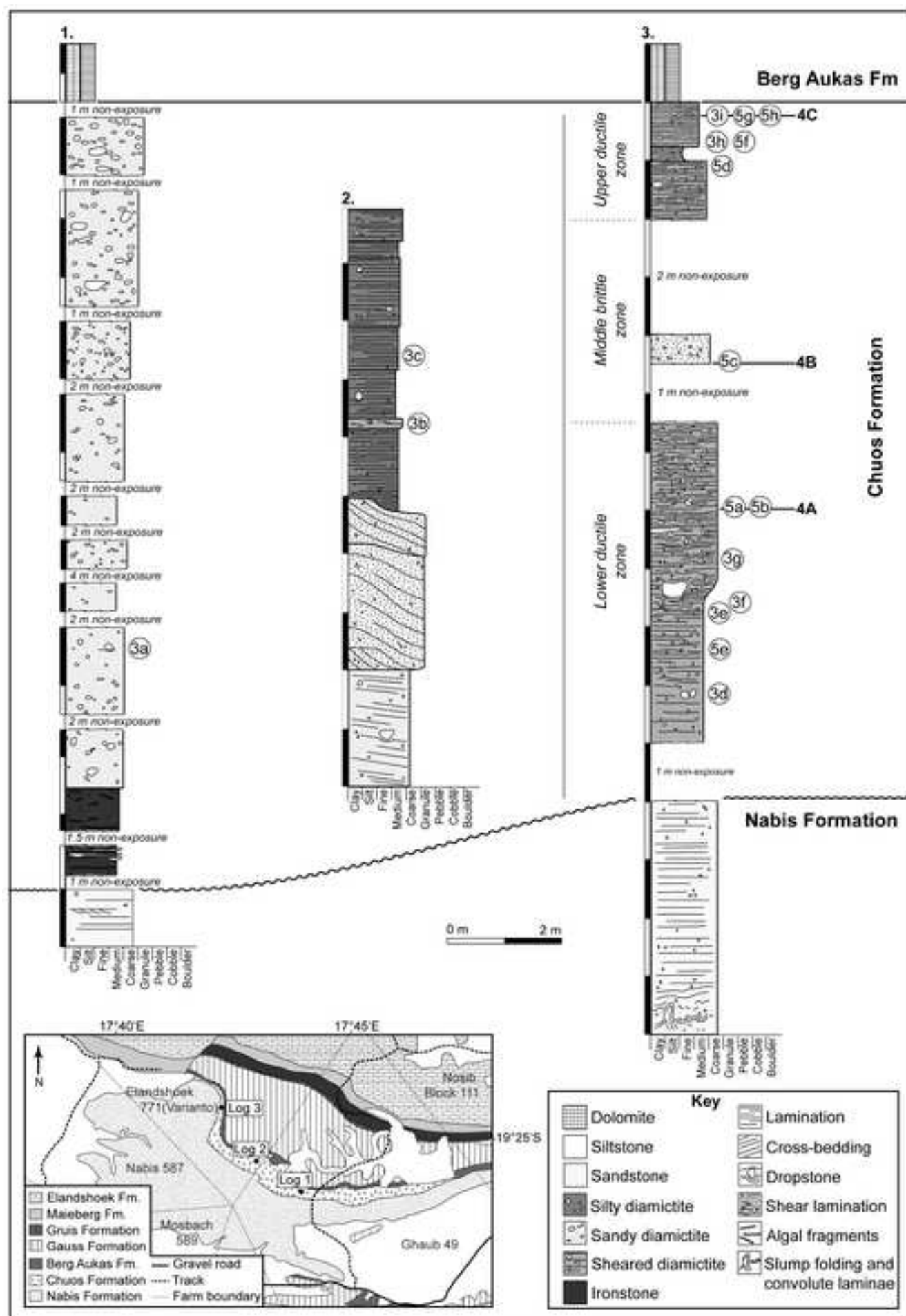
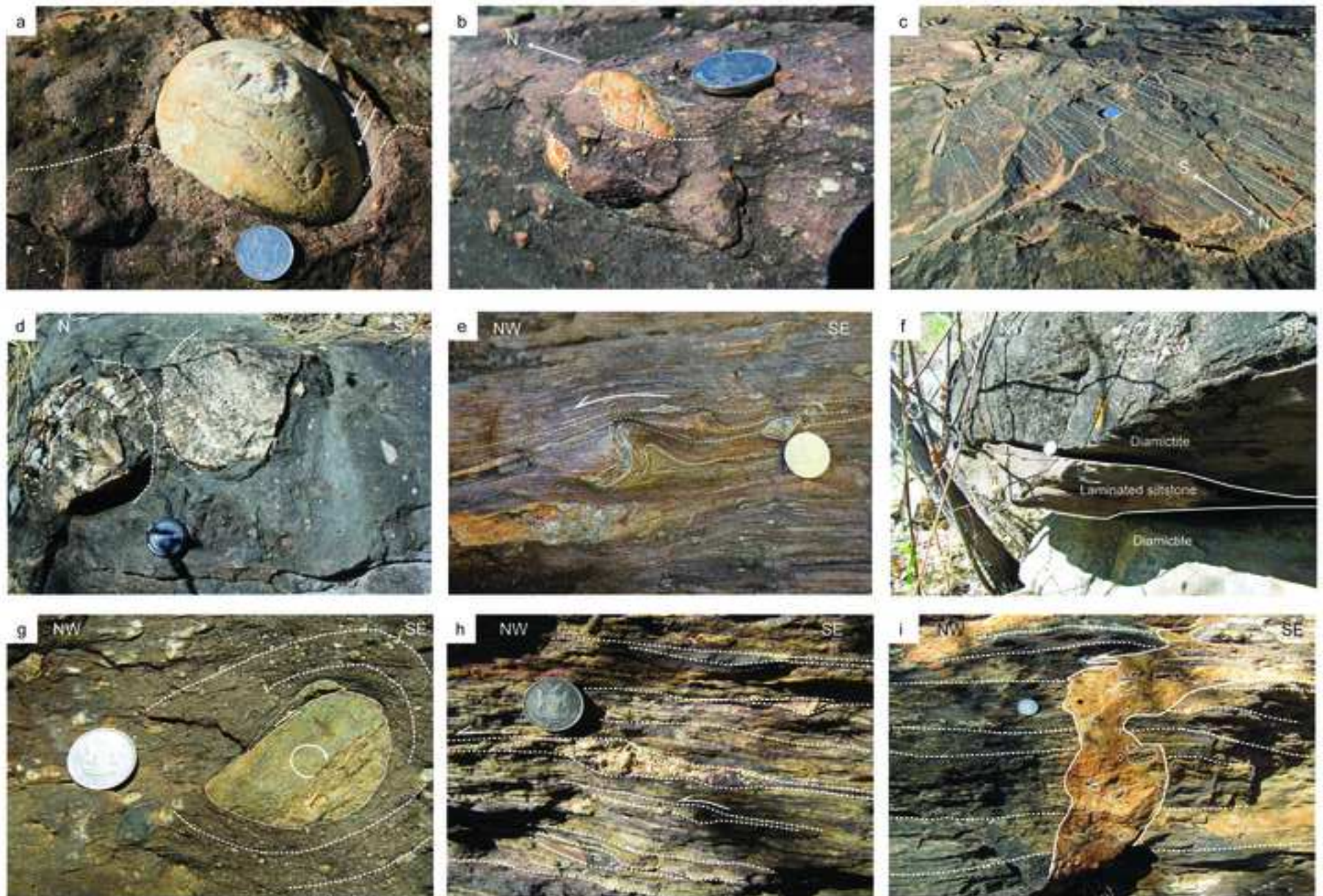


Figure
[Click here to download high resolution image](#)



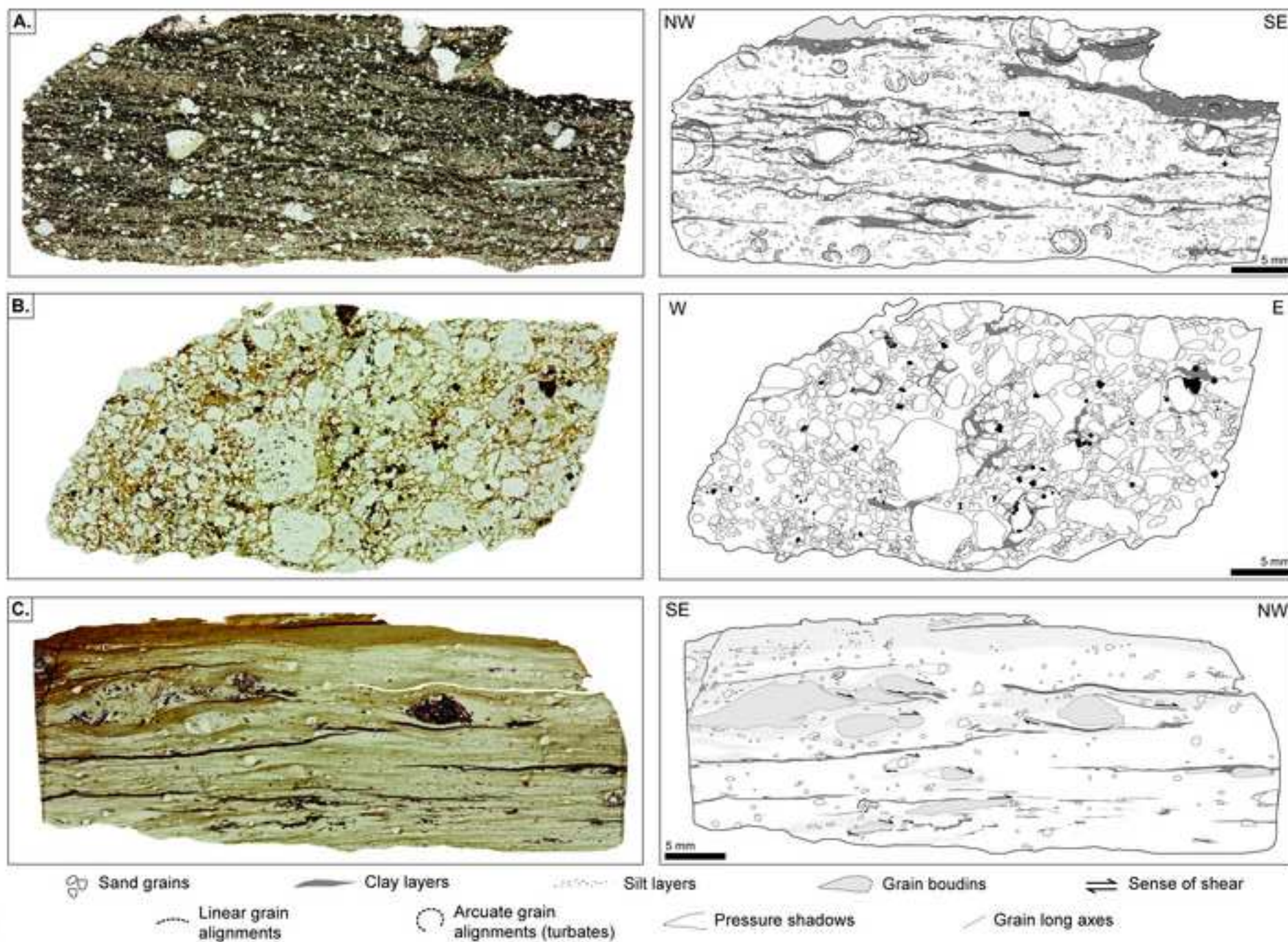
Figure

[Click here to download high resolution image](#)



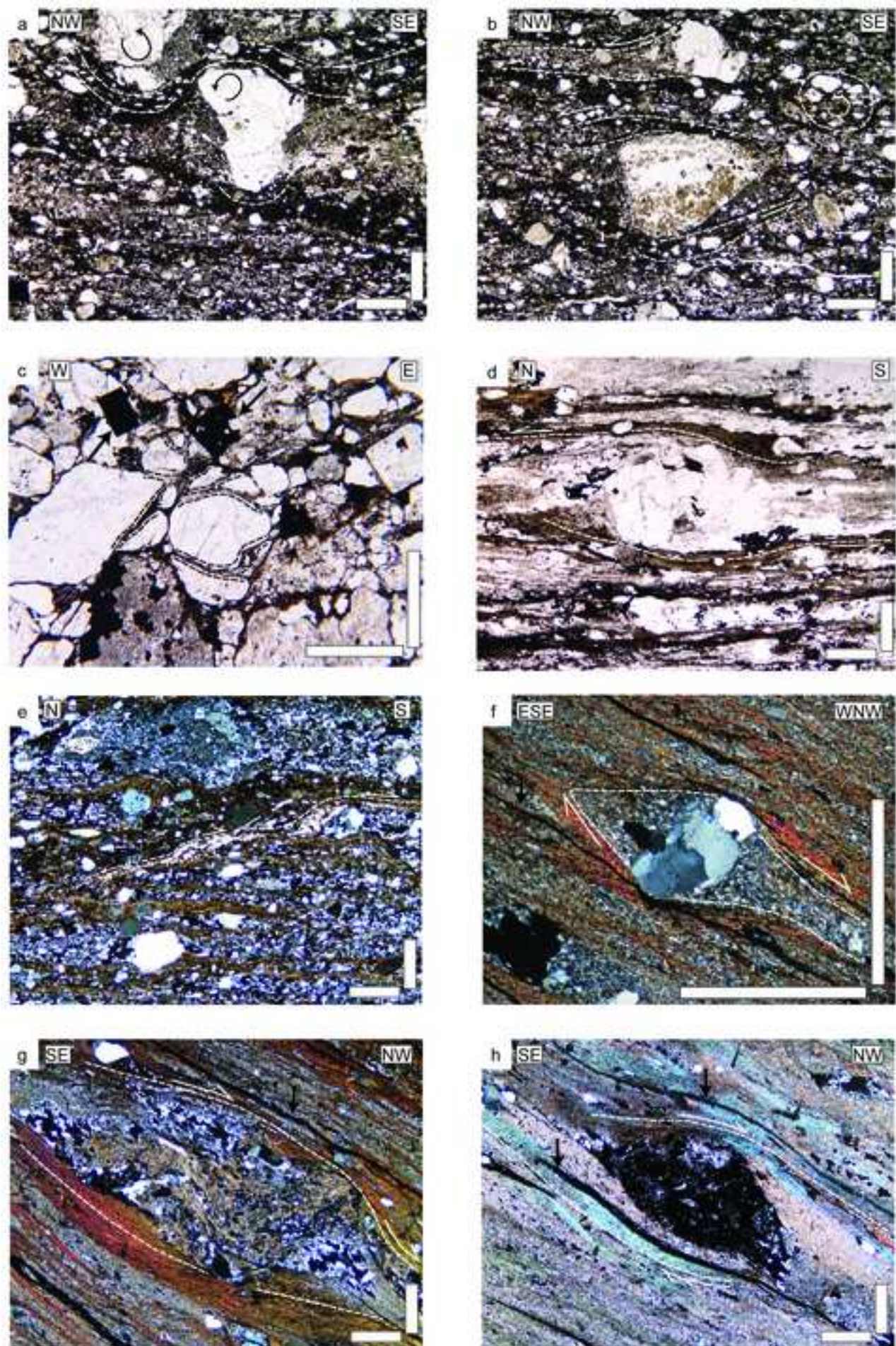
Figure

[Click here to download high resolution image](#)



Figure

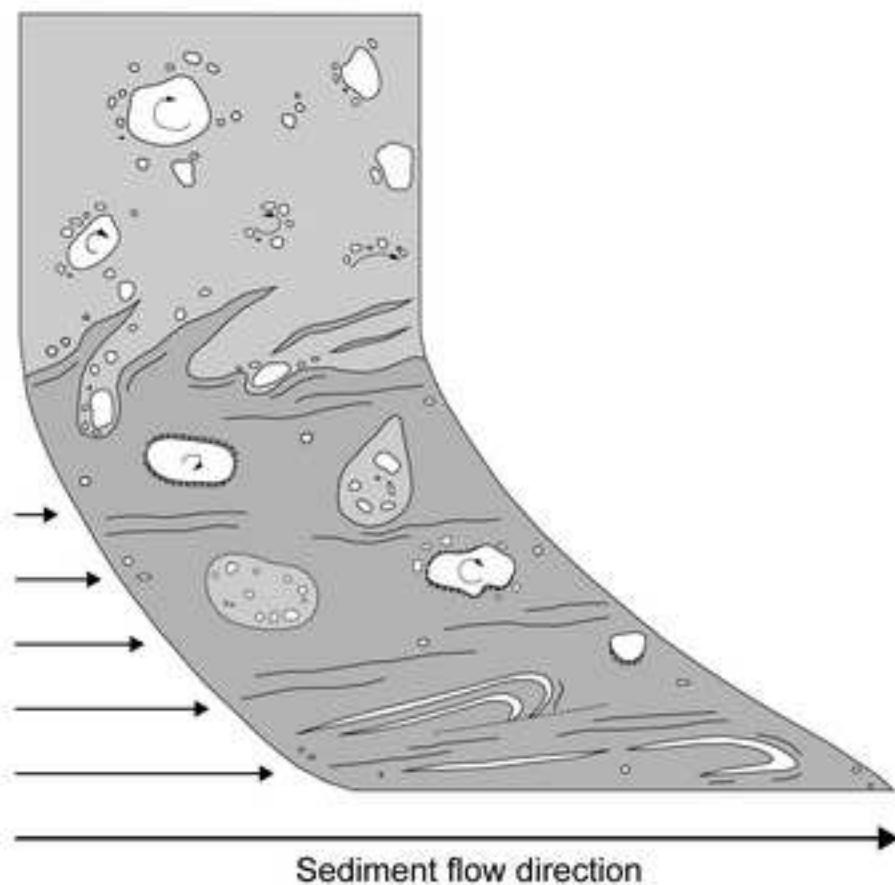
[Click here to download high resolution image](#)



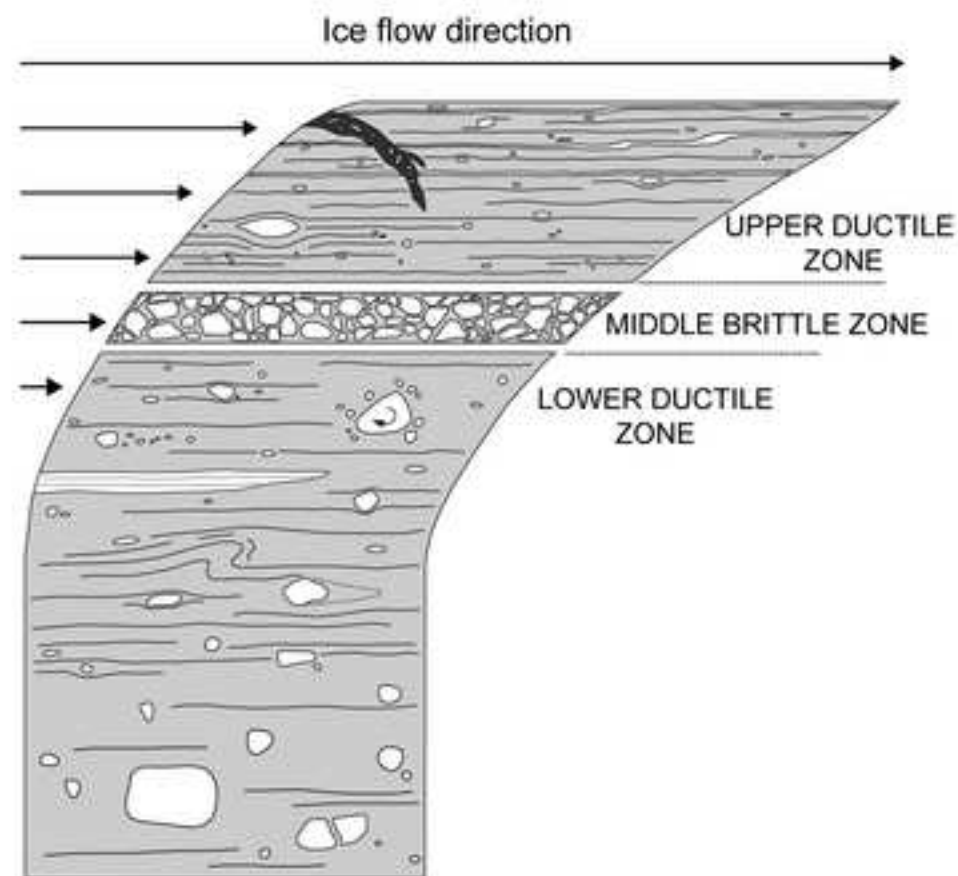
Figure

[Click here to download high resolution image](#)

1. Sediment gravity flow



2. Chuos Formation



- Diamicton
- Siltstone
- Carbonate

- Clastic grains
- Intraclasts (diamicton 'pebbles')

- Arcuate grain alignments (turbates)
- Laminated clast coatings

- ≡ Lamination
- ◁ Pressure shadows

Figure

[Click here to download high resolution image](#)

